Int. J. Nanoelectronics and Materials **7** (2014) 1-7

Structural and optical studies of Eu^{3+} doped nanocrystalline tellurite glass

E. S. Sazali*, M. R. Sahar and S. K. Ghoshal

Advanced Optical Material Research Group, Department of Physics, Faculty of Science, Universiti Teknologi Malaysia, 81310, Skudai, Johor Bahru, Johor, Malaysia.

Abstract

A series of transparent glasses with composition (80-x) TeO_2 - 5 Na_2O – 15 MgO – (x) Eu_2O_3, over the concentration region of 0 to 2.5 mol% were obtained using conventional melt-quenching technique. The nanocrystalline glass samples were prepared by heating the as-cast glasses above the crystallization temperature. The amorphous nanocrystalline and crystallized glass samples were characterized using X-ray diffraction (XRD). Scanning Electron Microscopy (SEM) was used to find the nano nature of the crystallinity. In addition, the optical properties were measured employing room temperature Photoluminescence (PL) spectroscopy. XRD spectra confirmed the mixed amorphous and crystalline nature of the glass. SEM studies revealed the nanocrystal glass morphology associated with the existence of crystalline phase. The influence of heat treatment process on the luminescence properties was performed in detail. The observed emission peaks for the luminescence such as $^5D_0 \rightarrow {}^7F_0$, $^5D_0 \rightarrow {}^7F_1$, $^5D_0 \rightarrow {}^7F_2$, $^5D_0 \rightarrow {}^7F_3$ and $^5D_0 \rightarrow {}^7F_4$ were found to be located at around the wavelength of 568 nm, 600 nm, 628 nm, 664 nm and 712 nm respectively. The enhancement of Eu^{3+} luminescence especially for the highest emission intensity, $^5D_0 \rightarrow {}^7F_2$ transition lies in the red region as compared to the precursor glass. Our findings may provide some useful information towards the development of functional glasses with controlled structural and optical properties.

Keywords: Nano-crystalline glass, XRD, SEM, Photoluminescence, FWHM, Inverse quality factor.

1. Introduction

Interest in tellurite glass containing rare earth element are expected for nonlinear optical devices as for their large third-order nonlinear optical susceptibility [1]. Moreover, the assimilation of rare earth ions can stabilize the metastable crystalline phase which leads to a development of optical devices based [2, 3]. Among all glasses, the Eu^{3+} doped tellurite glass arise great attention as they can perform persistent spectral hole burning in the $^7F_0 \rightarrow {}^5D_0$ transition [4]. The Eu^{3+} ion is also used as a probe for finding the local structure around the rare earth ion in a crystal or a glass due to relative simplicity of its energy level structure with non-degenerate ground $^7F_0$ and emitting $^5D_0$ states [5].

*) For correspondence, E-mail: mrahim057@gmail.com

Previously, there are many studies succeeded in fabricating transparent glass ceramic of tellurite based-glass system [3]. However, the synthesis of nano-crystalline Eu^{3+} doped TeO_2 based glass has been less extensive reported and the growth dynamic of the glass system is unclear [6]. According to the previously reported phase diagrams, the tellurite glasses can easily be obtained with a high concentration of europium [7]. Moreover, properties of Eu^{3+} doped TeO_2 glasses which undergo heat treatment process were studied only recently. Therefore, the aims of this study are to prepare the tellurite glass doped with europium (Eu^{3+}) via melt quenching technique. The effect of dopant throughout all samples towards the structural in terms of XRD and SEM will be investigated. In addition, the optical properties were determined with luminescence.

2. Experiment

The ability of glasses for crystallization was first measured by the values of the glass crystallization temperature (T_c) to obtain transparent glass ceramics. Portions of the glass sample were heat treated for 30 minutes at temperature 15 – 20^oC above the T_c in an electric furnace throughout all samples.

The XRD peak corresponding to be (111) plane where the particle size with basically a cubic structure was estimated from the full width at the half maximum (FWHM), β of an XRD peak corresponding to the plane shown by Scherrer's equation as shown in Eq.1.

$$d = 0.89 \lambda / \beta \cos \theta \quad (1)$$

where d is the crystallite size, λ is the wavelength and θ is the diffraction angle.

XRD measurement is performed on Siemens Diffractometer D5000. For this measurement, the samples must be in powder form. Diffraction patterns were collected in the 2θ range from 15 ^{o} to 75^o, in steps of 0.05^o and 1s counting time per step and using Cu Kα as a radiation source of wavelength λ=1.54056Å.

To investigate the kind of the formed crystallites, it was examined by SEM. The crystallized portion of glass was polished and then successively diamond paste. The specimen is then was coated with a thin layer of carbon by an evaporation technique. An electron accelerating voltage of 8 kV was used and the micrographs were obtained using back-scattered imaging.

The Photoluminescence measurement is conducted on Nanosecond Luminescence Spectroscopy System, Ekspla Model NT340/1 tunabled Nd: YAG laser system. Each sample which is in powder form was placed in the spectrometer and scanned for radiation spectral wavenumber in the range of 200 – 900 cm^{-1} at room temperature. The Xenon lamp ($300 < \lambda < 1300nm$) was used as a pumping source.

3. Results and Discussion

A series of unheat-treated and heat-treated TeO_2 - Na_2O – MgO glass system doped with Eu^{3+} have successfully been prepared by melt-quenching technique.

3.1 X-ray Diffraction

All the heat-treated samples are visually transparent. Fig. 1 reveals the XRD pattern for TeO_2 – Na_2O – MgO glass with 1.5 mol% Eu_2O_3 dopant concentrations which shows the reflections expected from crystalline particles after heat-treatment. The XRD pattern reveals the presence of α-TeO_2 and γ-TeO_2 structures.

The particle size of crystalline phase was estimated from the (FWHM) as shown in Fig.1. Using Scherrer's equation describe in Eq.1, the average of crystallite size are estimated to be 68.7 nm. The diffraction angle values (2θ) of 28.8°, 35.4°, 40.1°, 44.6°, 55.2° and 61.0° confirm the presence of the α-TeO_2 phase (paratellurite) and γ-TeO_2 phase [8]. It indicates that the presence of TeO_2 might play a major role in the phase formation. Indeed the crystallites are nanosized particles.

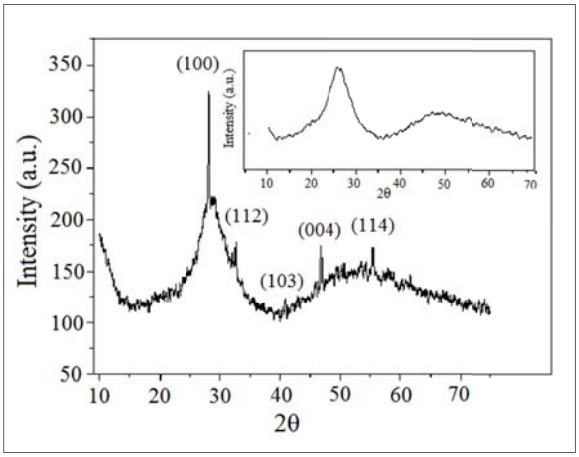

Fig. 1: XRD spectra at room temperature for 78.5 TeO_2 – 5 Na_2O – 15 MgO – 1.5 Eu_2O_3 glass after heat-treatment at 442.7°C. The inset shows the XRD patterns for the same glass in the as-cast condition.

3.2 Scanning Electron Microscopy

The existence of crystalline phase was verified by SEM analysis. Fig. 2(a)-(d) show the SEM micrographs of some TeO_2 – Na_2O – MgO glass systems in varying Eu_2O_3 dopant concentration. Some of them are spherical in shape, some have star-like structure and some of them are irregular in shape. All the micrographs confirm that the crystalline region is composed of TeO_2 phase is dominant.

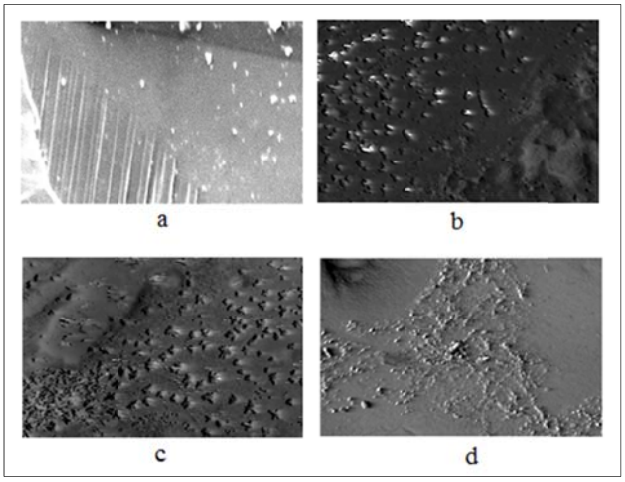

Fig. 2: SEM pictures obtained for heat-treated Eu_2O_3 (x) doped glass system above T_c with (a) x = 0, (b) x = 0.5, (c) x = 1.0 and (d) x = 2.0.

Throughout the heat-treated of samples, although the nucleation and growth of nano-crystalline are developed in the same heat-treat operation, but the distribution of nucleates and growth of crystal cannot attain the same extent as the dopant concentration is different. This shows the incorporation of Eu^{3+} dopants with the synthesis of nano-crystalline TeO_2 – Na_2O – MgO glass system. Crystal immersed in the amorphous material, with no observable clustering and a size distribution of are observed.

3.3 Photoluminescene Spectra

Luminescence is the capability of materials to absorb energy and reemitting visible light [9]. Fig. 3 shows the luminescence spectra of Eu^{3+} doped TeO_2 – MgO – Na_2O for heat-treated glass system where the dopant concentration value is varied from 0.5 mol% to 2.5 mol%, respectively. Five emission bands corresponding to $^5D_0 \rightarrow {}^7F_0$, $^5D_0 \rightarrow {}^7F_1$, $^5D_0 \rightarrow {}^7F_2$, $^5D_0 \rightarrow {}^7F_3$ and $^5D_0 \rightarrow {}^7F_4$ are evidenced with an excitation wavelength λ_{exci} = 400 nm. From previous work, the identified excitation bands for those transitions are around 355 nm to 395 nm as summarized in Table 1 [4, 5, 10]. The emission lines belong to transitions between the energy levels of the $4f^6$ configuration of Eu^{3+} ion. The obtained emission peaks of Eu^{3+} doped tellurite glass system at the corresponding transitions cofirmed the presence of europium trivalent state in this glass system which may present large luminescene efficiency [11].

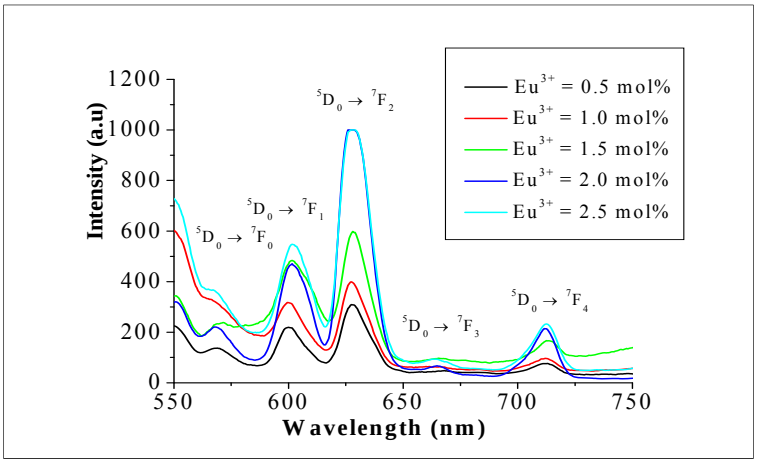

Fig. 3: A luminescence spectra of Eu^{3+} doped TeO_2 - Na_2O - MgO for heat-treated glass system excited at 400 nm.

Fig. 4 shows the luminescence spectra of the 1 mol% Eu_2O_3 concentration for the unheat-treated and heat-treated glass sample at temperature above the crystallization temperature (T_c) for 30 minutes. The detected emission spectra for heat-treated glass sample with the same Eu_2O_3 concentration is similar to the as-cast glass sample, which contributes to the same transition. It is clearly be seen that the shape of emission band does not change but there is a slightly shift of the peaks position which indicates the interaction of ions between Eu^{3+} sites is very strong [12]. Both of them exhibit the same five emissions which are in agreement with the other researcher [11].

From Fig. 4, it is clear that both unheat-treated and heat-treated glass show about similar emission wavelength throughout five emissions transitions. It can be explained by the energy of photon emitting which does not influenced by Eu_2O_3 concentration. In consequents, the number of photon emitted is really affected the intensity of the emissions as the concentration of Eu_2O_3 is very sensitive to them. Moreover, it can be concluded that the samples are very stable since its energy remains at the same transition level as the dopant concentration is varied.

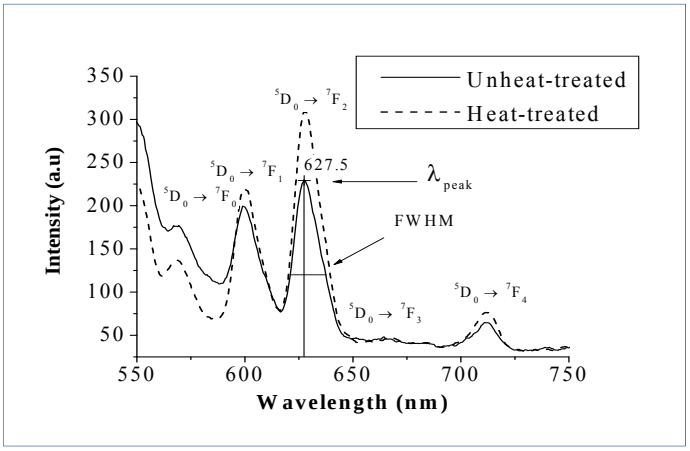

Fig. 4: Emission Spectra of glass at 1 mol% of Eu_2O_3 for unheat-treated and heat-treated glass.

By taking the average peak wavelength throughout all samples, a plot of peak wavelength as a function of different transitions for both untreated and heat-treated glass sample as illustrated in Fig. 6. The observed peak wavelength throughout all emission peaks for $^5D_0 \rightarrow {}^7F_0$, $^5D_0 \rightarrow {}^7F_1$, $^5D_0 \rightarrow {}^7F_2$, $^5D_0 \rightarrow {}^7F_3$ and $^5D_0 \rightarrow {}^7F_4$ is found to be at around 568 nm, 600 nm, 628 nm, 664 nm and 712 nm, respectively. As we can see, the average transition of $^5D_0 \rightarrow {}^7F_0$ emits in the lower wavelength at 568 nm, which was describe as yellow region. Peak wavelength of $^5D_0 \rightarrow {}^7F_1$ transition is in the orange region which is at 600. For the highest emission intensities of $^5D_0 \rightarrow {}^7F_2$ transition lies in the red region at 628 nm. The color region is then consistently in red region for $^5D_0 \rightarrow {}^7F_3$ and $^5D_0 \rightarrow {}^7F_4$ transitions at 664 nm and 712 nm, respectively.

By taking the average peak intensity throughout all samples, a plot of peak intensity as a function of different transitions for both untreated and heat-treated glass sample as illustrated in Fig. 5 for all Eu_2O_3 concentration. The experimental data is further compared with the intensity of luminescence emission spectra with heat-treated glass sample. It can be seen that the spectra of the samples present higher emission intensities with the heat-treatment process. As the glass undergoes heat-treatment process, the increase in the intensity of emission spectra is observed. This indicates that the local crystalline field symmetry around the Eu^{3+} ions does change due to the heat-treatment. Therefore, the mechanisms that are contributing for changes in the intensity of the Eu^{3+} emissions in samples are due to the heat treatment process. In addition, with heat-treatments, all emissions transitions are due to the transition from a glass-like to a crystal-like environment [10].

It is observed that the emission located at around 620 to 630 nm are more affected with the heat-treatment process as the peak intensity of $^5D_0 \rightarrow {}^7F_2$ at 627.5 nm is the highest if compared to the others transition and $^5D_0 \rightarrow {}^7F_3$ shows the weakest transition. The highest transition, $^5D_0 \rightarrow {}^7F_2$ transition with electric dipole ($\Delta J = 2$) have the maximum europium intensity which is about two times higher from $^5D_0 \rightarrow {}^7F_1$ with electric dipole transition ($\Delta J = 1$). According to Giridhar *et.al,* (2000), these two transitions are the spin forbidden emission bands with ($\Delta S = 1$). Transitions $^5D_0$–$^7F_2$ is electric-dipole allowed and therefore their amplitudes are sensitive to changes in the polarizability of the ligand and reduction of the local symmetry around the Eu^{3+} ions [11].

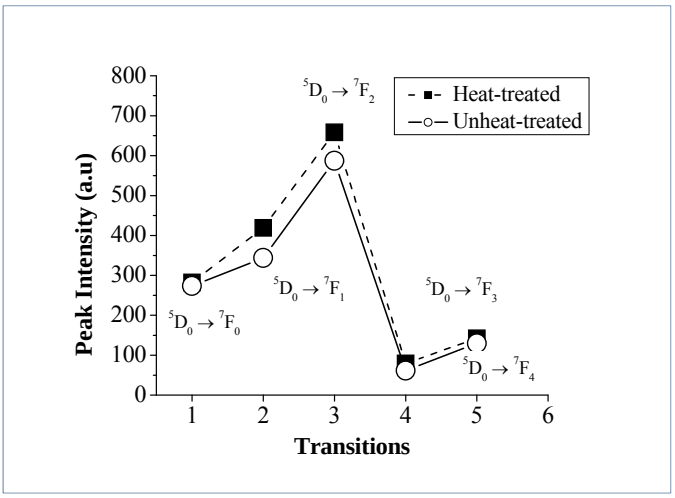

Fig. 6: Peak intensity as a function of different transitions.

4. Conclusion

A series of glass system based on (80-x) TeO_2 - $5Na_2O$ - 15MgO - (x) Eu_2O_3 for both unheat-treated and heat-treated or nano glass system over the concentration region from 0 to 2.5 mol% have successfully been obtained using conventional melt quenching technique. The series of glasses shows a good quality of glass as they are largely transparent and visualized.

For the crystallization investigation, XRD spectra confirms the presence of crystalline phase of nano glass which the diameter is estimated around 68.7 nm and SEM studies revealed the nano-crystal glass morphology which is associated to the existence of crystallized phase. Crystal immersed in the amorphous material, with no observable clustering and a size distribution of are observed.

A detailed study of on the luminescence properties has successfully been carried out. The result shows some peak observed throughout all emission peaks for $^5D_0 \rightarrow {}^7F_0$, $^5D_0 \rightarrow {}^7F_1$, $^5D_0 \rightarrow {}^7F_2$, $^5D_0 \rightarrow {}^7F_3$ and $^5D_0 \rightarrow {}^7F_4$ was found to be at around 568 nm, 600 nm, 628 nm, 664 nm and 712 nm, respectively. The enhancement of Eu^{3+} luminescence especially for the highest emission intensity, $^5D_0 \rightarrow {}^7F_2$ transition which lies in the red region as compared to the precursor glass is exhibited.

Acknowledgments

The authors gratefully acknowledge the financial support from Ministry of Higher Education through grant Vot. 4F083 and Universiti Teknologi Malaysia under Vot. 02J77 (GUP/MOHE) and MyMaster.

References

[1] J. S. Wang, E.M. Vogel, E. Snitzer, J. Non-Cryst. Solids, **178** (1994) 109

[2] J. Matthew, Dejneka, Alexander Streltsov, Science and Technology Division, Corning Incorporated, Corning, NY 14831 (2002)

[3] K. Hirano, Y. Benino, T. Komatsu, J.Phys. Chem.of Solids **62** (2001) 2075

[4] P. Giridhar, S. Sailaja, M. Bhushana Reddy, K. Vemasevana Raju, C. Nageswara Raju, B. Sudhakar Reddy, B, Ferroelectrics Letters, **38** (2011) 1

[5] P. Babu, C. K. Jayasankar, Physica **B 279** (2000) 262

[6] V. Ravi Kumar, V. Bhatnagar, K. Anil, R. Jagannathan, *Structural and Optical Studies of Pr^{3+}, Nd $^{3+}$ and Eu^{3+} Ions in Tellurite Based Oxyfluride, TeO_2-Cif Glasses* (2001)

[7] T. Watanabe, Y. Benino, K. Ishizaki, T. Komatsu, J. Ceram. Soc. Japan. **107** (2000) 1140

[8] Burcu Oz, Thermal Microstructural and Optical Characterization of TeO_2-K_2O Glasses (2006)

[9] W. D. Callister Jr., *Materials Science and Engineering: An Introduction*, John Wiley and Sons, Inc, New York (1985)

[10] R. P. Luciana, Kassab, Ricardo de Almeida, M. Davinson da Silva, A. A. Thiago De Assumpçao, Cid B. D Araújo, J. Appl. Phys. **105** (2009) 103505

[11] Budi Astuti, Study of Optical Properties of P_2O_5 – Sm_2O_3 – MnO_2 Glass System, Universiti Teknologi Malaysia (2005)